Hydrogen Bond Rearrangements in Organic Solids. Part 2.[1] Cyclodehydration of *o*-Acetamidobenzamide

Margaret C. Etter
3M Central Research Laboratories, St. Paul, Minnesota 55133, U.S.A.

o-Acetamidobenzamide (I) undergoes a series of thermal solid-state rearrangements in which a polymorphic transformation and cyclodehydration occur to give anhydrous 2-methylquinazol-4-one (IV). The solid-state processes involved in cyclodehydration of (I) have been investigated. An important feature of this reaction sequence is that it occurs in a matrix of hydrogen-bonded molecules. The hydrogen-bonding patterns, which may play a role in directing the solid-state transformations, are used as a probe for understanding the solid-state reaction mechanisms. The *X*-ray crystal structures of (IV), and its hydrate (III) were solved, and are compared with those of (I). Crystal data: (IV), *Pbca*, a = 5.081(6), b = 14.574(7), c = 20.854(3) Å, Z = 8, R_F = 0.075 for 622 reflections [$I > 3\sigma(I)$]; (III), $P\bar{1}$, a = 10.000(3), b = 12.509(4), c = 7.193(3) Å, α = 78.26(3)°, β = 79.05(3)°, γ = 89.87(3)°, Z = 4, R_F = 0.070 for 1 346 reflections [$I > 3\sigma(I)$].

While the importance of hydrogen bonds in determining crystal packing patterns of carboxylic acids and amides has been well established,[2,3] their role in the solid-state transformations of these compounds is not so well understood. In a previous paper [1] we reported the solid-state chemistry involved in a multistep reaction in which the diamide (I) undergoes competing hydrogen-bond rearrangements. It was shown that *o*-acetamidobenzamide, (I), is transformed thermally into 2-methylquinazol-4-one, (IV).[1] The reactions in Scheme 1 were proposed. The hydrogen bond changes involved in the reaction (A) ⟶ (B) were described, and the differential scanning calorimetry (d.s.c.) behaviour of (B) as it is transformed into (D) was presented. An in termediate (C) was identified by the appearance in d.s.c. scans of a species with a reduced m.p. [*ca.* 30 °C lower than the m.p. of (B), and 80 °C lower than that of (D)]. Species (C) appears reproducibly upon heating independent samples of (B), although its m.p. varies by ±10 °C. The formation of (C), however, is not reversible, since continued heating converts the sample entirely into (D). Compounds (II) and (III) were proposed as reasonable chemical intermediates which might be present in (C) and thereby account for the d.s.c. results. This paper deals with the identification of (C), and clarification of the solid-state processes, in particular the hydrogen bond rearrangements, during conversion of (B) into (D). The crystal structures of (D) and its hydrate (E) were solved in order to identify their hydrogen bonding patterns and their relationship in the mechanism.

In general, solid-state chemical reactions encompass both packing pattern changes (*e.g.*, polymorphic transformations or loss of water of hydration), as well as formation of new molecular species (analogous to chemical reactions in solution). A particular molecule can, in fact, be both the reactant and the product in a solid-state reaction. Likewise, a solid-state species could contain more than one kind of molecule. Thus, it becomes important in a discussion of solid-state reaction mechanisms to distinguish clearly between a molecular species and a solid-state species. In this paper this distinction is emphasized by referring to molecular species with Roman numerals, and to solid-state species with capital letters.

Experimental

Crystal Properties and Preparation.—The preparation of two polymorphs of (I) was described previously.[1] Compound (IV) can be obtained by Scheme 1, but for crystal analysis it was prepared independently by refluxing (I) in water or in aqueous $NaHCO_3$ solution.[4] The precipitate, m.p. 240 °C, can be recrystallized from water to give clear plate-like crystals (E) which are the hydrated quinazolone (III). Thermogravimetric analysis (t.g.a.) of these crystals shows a 10% weight loss at 90 °C, corresponding to quantitative loss of 1 mole of water giving (D). The sample can be alternatively dehydrated by heating overnight at 60 °C to give microcrystalline (D). [Single crystals of (E) lose water slowly under ambient conditions and the crystals appear speckled.] The i.r. spectra of (D) and (E) (Figure 1) show differences in the OH region of the spectrum, a carbonyl band shift from 6.05 μm in (E) to 5.90 μm in (D), and a new broad band at 11.2 μm for (D).

Subliming the hydrate (E) at 90 °C gives large crystals of anhydrous (IV) which have the same m.p. and i.r. pattern as independently prepared samples of (D.)

Structure Determinations.—Data for both structures were collected on a Nonius CAD-4 diffractometer. The crystal of (E) was coated with epoxy-cement to retard dehydration. Measurements of the intensities of several check reflections during the data collection for (E) showed that there was only a few percent loss in intensity. Crystal data are listed in Table 1, and data collection details in Table 2. Both structures were

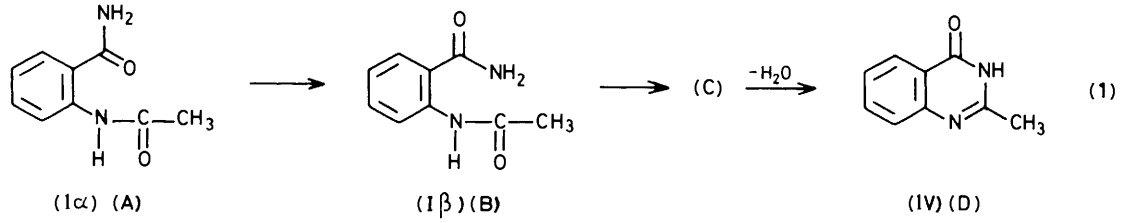

Scheme 1

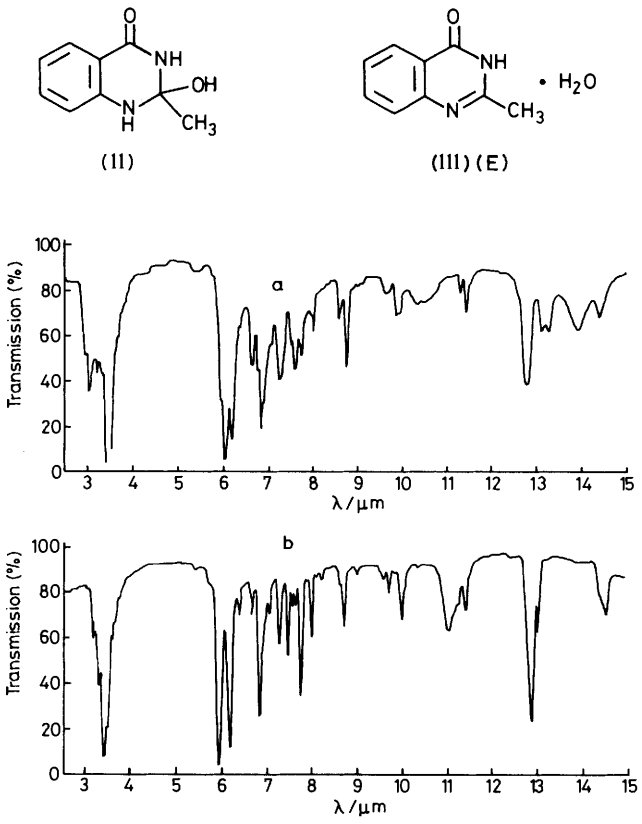

Figure 1. I.r. spectra (Nujol) of (a) the quinazolone hydrate (E) before heating, and (b) anhydrous quinazolone (D) obtained by heating the hydrate at 60 °C overnight

solved using the MULTAN direct methods procedures from the Nonius Structure Determination Package.[5] *E* maps computed from models with the highest figures of merit revealed the positions of the non-hydrogen atoms. The hydrogen atoms were located using difference Fourier maps, and their parameters included in the final least squares refinements. Using isotropic thermal parameters for the hydrogen atoms and anisotropic thermal parameters for the heavy atoms convergence was reached at $R = 0.075$ and $R_w = 0.078$ for (D), and $R = 0.070$ and $R_w = 0.070$ for (E). The final atomic co-ordinates are listed in Table 3. A full list of final refined parameters, e.s.d.s, observed bond lengths and angles, and structure factors are contained in Supplementary Publication No. SUP 23444 (37 pp.).* Selected bond lengths and angles are given in Table 4.

Solid-state Reactions.—(B) ⟶ (D). Several processes occur simultaneously during the transformation (B) ⟶ (D). If (B) is heated to 180 °C and maintained at that temperature for *ca.* 1 h, then cooled to room temperature and reheated, the only endotherm observed is due to the melting of (D) at 240 °C. On the other hand, if (B) is heated just until it melts, is rapidly cooled, and reheated, then a new endotherm (*ca.* 6 kcal mol^{-1}) due to (C) is seen at 150—160 °C. After one or two cycles of heating and cooling, this endotherm disappears and, again, only the melt of (D) is detected. The solid-state species (C) could be either a new molecular species, *i.e.*, an intermediate in the reaction of (I) ⟶ (IV), or a new solid-state

* For details of Supplementary Publications see Notice to Authors No. 7 in *J. Chem. Soc., Perkin Trans. 2*, 1981, Index Issue.

Table 1. Crystal data

	(IV) (D)	(III) (E)
Formula	$C_9H_8N_2O$	$C_9H_{10}N_2O_2$
Molecular wt.	160.2	178.2
Space group	*Pbca*	$P\bar{1}$
a (Å)	5.081(6)	10.000(3)
b (Å)	14.574(7)	12.509(4)
c (Å)	20.854(3)	7.193(3)
α (°)	90	78.26(3)
β (°)	90	79.05(3)
γ (°)	90	89.87(3)
U/Å^3	1 545	864.3
Z	8	4
D_c/g cm^{-3}	1.38	1.37

Table 2. Data collection

	(D)	(E)
Crystal size (mm)	0.4 × 0.12 × 0.08	0.2 × 0.04 × 0.04
μ/cm^{-1}	7.7	1.0
Radiation (graphite monochromator)	Cu-K_α (1.541 78 Å)	Mo-K_α (0.710 69 Å)
2θ limit (°)	150	50
No. unique reflections	1 519	3 028
No. observed reflections $I > 3\,\sigma(I)$	622	1 346
Weighting scheme	unit weights	unit weights
R_w *	0.078	0.070
R_F *	0.075	0.070

* $R_w = \frac{\Sigma w(|F_o| - |F_c|)^2}{\Sigma w F_o^2}$, $^2R_F = \frac{\Sigma||F_o| - |F_c||}{\Sigma|F_o|}$

composition, which is an intermediate in the reaction (B) ⟶ (D). Compound (II), considered as a chemically reasonable molecular intermediate, is probably formed as a transient species but we have been unable to document its formation by any chemical or spectroscopic means. An alternative possibility is that (III) forms and nucleates the growth of (E). To investigate the possibility that (C) is actually crystalline (III), crystals of (E) were prepared *from solution* and their solid-state properties investigated.

(E) ⟶ (D).—(E) readily dehydrates to give (D) upon heating, as shown in the differential thermal analysis (d.t.a.) curves in Figure 2. The large endotherm at 110 °C is due to the loss of water (corroborated by t.g.a.). Upon cooling and reheating the sample, this endotherm is no longer present and only the melt endotherm due to (D) is seen.

I.r. spectra and *X*-ray powder patterns were examined at various stages of heating (B). We found no evidence for (III), or for (E), or for the presence of significant amounts of water in the solid-state samples. Since water must be forming during cyclodehydration, it is most likely being driven off from the solid as rapidly as it is formed. A careful examination of the original d.s.c. curves of (B)[1] shows a reproducible endotherm (2 kcal mol^{-1}) occurring slowly over a broad temperature range between 100 and 150 °C, probably due to loss of water from the sample. (E) shows no endotherm of the magnitude or sharpness of the one seen in the d.s.c. curves of (C), at 150—160 °C.[1]

(F) ⟶ (D).—An unusual solid-state species (F), made by recrystallizing (I) from hot aqueous $NaHCO_3$, shows thermal behaviour remarkably similar to that of (C). This sample has an initial endotherm also *ca.* 30 °C below the m.p. of B, followed by resolidification of the sample and melting at 240 °C. *X*-Ray Weissenberg patterns for several single crystals

Table 3. Positional and thermal parameters and their estimated standard deviations

Anhydrous quinazolone (IV)

Atom	*x*	*y*	*z*	*B*(1,1)	*B*(2,2)	*B*(3,3)	*B*(1,2)	*B*(1,3)	*B*(2,3)
O(1)	0.747(1)	0.086 6(2)	−0.008 6(1)	0.048(3)	0.006 8(2)	0.001 7(6)	−0.001(2)	0.002(1)	0.000 3(2)
N(1)	0.821(1)	−0.008 0(3)	0.076 0(2)	0.033(3)	0.005 3(2)	0.001 36(7)	0.002(2)	0.002(1)	−0.000 7(2)
N(2)	0.574(1)	−0.004 8(3)	0.171 3(2)	0.049(4)	0.005 4(2)	0.001 28(7)	−0.001(2)	0.002(1)	0.000 2(2)
C(1)	0.330(2)	0.178 9(3)	0.063 3(2)	0.045(4)	0.005 6(2)	0.001 44(9)	−0.003(2)	−0.003(1)	0.000 0(3)
C(2)	0.139(2)	0.217 2(3)	0.100 9(2)	0.044(4)	0.005 0(3)	0.001 97(11)	0.006(2)	0.000(2)	0.000 3(3)
C(3)	0.096(2)	0.180 9(3)	0.162 0(2)	0.033(4)	0.005 6(3)	0.001 97(11)	0.002(2)	−0.002(2)	−0.001 2(3)
C(4)	0.232(2)	0.107 5(3)	0.183 4(2)	0.035(4)	0.005 6(3)	0.001 50(9)	−0.001(3)	0.001(1)	0.000 0(3)
C(5)	0.432(1)	0.067 9(3)	0.146 0(2)	0.032(3)	0.004 4(2)	0.001 18(8)	−0.001(2)	−0.002(1)	−0.000 2(3)
C(6)	0.481(2)	0.104 6(3)	0.084 8(2)	0.040(4)	0.004 8(2)	0.001 12(8)	−0.002(2)	0.000(1)	−0.000 6(3)
C(7)	0.689(2)	0.062 5(3)	0.047 0(2)	0.040(4)	0.005 0(2)	0.001 31(8)	−0.004(2)	−0.001(1)	−0.000 6(3)
C(8)	0.760(2)	−0.038 8(3)	0.137 3(2)	0.033(3)	0.004 9(2)	0.001 52(9)	−0.003(2)	0.000(1)	−0.000 4(3)
C(9)	0.926(2)	−0.114 8(4)	0.161 4(2)	0.040(4)	0.005 7(3)	0.002 41(13)	0.005(2)	0.003(2)	0.000 6(4)
H(1)	0.22(2)	0.080(2)	0.227(2)	5.(1)					
H(2)	−0.07(2)	0.209(3)	0.181(2)	7.(2)					
H(3)	0.06(1)	0.271(2)	0.088(2)	3.(1)					
H(4)	0.37(1)	0.195(2)	0.020(2)	6.(1)					
H(5)	1.01(1)	−0.032(2)	0.060(2)	4.(1)					
H(6)	0.34(2)	0.400(3)	0.148(2)	8.(2)					
H(7)	0.62(2)	0.382(4)	0.200(3)	8.(2)					
H(8)	0.57(2)	0.332(3)	0.136(2)	7.(2)					

Quinazolone hydrate (III)

O(1)	0.980 5(5)	0.282 0(4)	0.895 2(8)	0.010 1(0)	0.004 1(0)	0.029 7(0)	0.001 2(0)	−0.014 1(0)	−0.005 8(0)
O(2)	0.452 2(5)	0.211 6(4)	0.169 9(9)	0.010 1(0)	0.005 3(0)	0.041 9(0)	−0.000 6(0)	−0.001 5(0)	−0.011 3(0)
O(3)	0.375 1(5)	0.683 0(4)	0.146 7(8)	0.009 2(0)	0.005 7(0)	0.028 4(0)	−0.002 5(0)	−0.007 6(0)	−0.006 1(0)
O(4)	0.075 9(5)	0.182 5(4)	0.230 6(9)	0.010 4(0)	0.005 3(0)	0.031 4(0)	0.003 0(0)	−0.009 9(0)	−0.004 4(0)
N(1)	0.313 8(6)	0.060 8(5)	0.246 1(9)	0.007 9(0)	0.004 4(0)	0.021 5(0)	0.001 6(0)	−0.000 3(0)	−0.004 6(0)
N(2)	0.387 7(6)	−0.118 6(5)	0.307 5(9)	0.006 8(0)	0.004 6(0)	0.019 4(0)	0.000 9(0)	−0.001 8(0)	−0.003 5(0)
N(3)	0.972 6(5)	0.608 5(4)	0.674 1(8)	0.005 7(0)	0.005 0(0)	0.017 5(0)	0.000 5(0)	−0.002 1(0)	−0.005 5(0)
N(4)	0.872 8(6)	0.432 1(4)	0.783 3(9)	0.007 4(0)	0.004 8(0)	0.017 6(0)	0.001 0(0)	0.000 1(0)	−0.006 4(0)
C(1)	0.442 4(8)	0.111 9(5)	0.210 3(11)	0.011 0(0)	0.003 7(0)	0.021 4(0)	−0.000 4(0)	−0.002 5(0)	−0.007 5(0)
C(2)	0.292 5(7)	−0.050 8(5)	0.289 8(11)	0.007 6(0)	0.003 5(0)	0.022 5(0)	0.001 2(0)	−0.006 8(0)	−0.007 8(0)
C(3)	0.520 4(7)	−0.074 6(5)	0.276 3(10)	0.007 6(0)	0.005 2(0)	0.014 6(0)	0.003 7(0)	−0.003 5(0)	−0.007 0(0)
C(4)	0.552 3(7)	0.037 1(5)	0.228 5(10)	0.008 2(0)	0.003 9(0)	0.017 2(0)	0.001 9(0)	−0.007 1(0)	−0.007 8(0)
C(5)	0.686 7(8)	0.077 9(7)	0.198 0(12)	0.008 5(0)	0.008 0(0)	0.028 5(0)	0.002 9(0)	−0.011 0(0)	−0.011 3(0)
C(6)	0.788 3(8)	0.003 8(7)	0.217 8(13)	0.008 5(0)	0.008 7(0)	0.029 3(0)	−0.000 7(0)	−0.010 1(0)	−0.009 5(0)
C(7)	0.757 9(8)	−0.108 4(7)	0.264 6(13)	0.011 4(0)	0.010 4(0)	0.028 0(0)	0.009 1(0)	−0.015 2(0)	−0.013 8(0)
C(8)	0.625 8(8)	−0.149 3(6)	0.296 6(12)	0.010 1(0)	0.005 8(0)	0.024 7(0)	0.001 3(0)	−0.007 9(0)	−0.006 0(0)
C(9)	0.868 4(7)	0.542 7(5)	0.710 8(9)	0.006 5(0)	0.004 6(0)	0.012 2(0)	0.003 8(0)	−0.004 2(0)	−0.005 7(0)
C(10)	0.985 6(7)	0.380 6(5)	0.830 4(10)	0.007 6(0)	0.003 9(0)	0.020 3(0)	0.004 8(0)	−0.007 6(0)	−0.007 6(0)
C(11)	1.105 1(6)	0.454 3(5)	0.794 0(10)	0.004 6(0)	0.005 0(0)	0.016 6(0)	0.002 9(0)	−0.006 3(0)	−0.007 6(0)
C(12)	1.094 3(7)	0.564 3(5)	0.715 1(10)	0.006 9(0)	0.004 4(0)	0.014 3(0)	−0.000 6(0)	−0.002 4(0)	−0.006 0(0)
C(13)	1.210 9(7)	0.634 4(6)	0.674 2(12)	0.008 2(0)	0.005 7(0)	0.025 5(0)	−0.001 2(0)	−0.007 0(0)	−0.006 0(0)
C(14)	1.332 4(8)	0.592 7(7)	0.715 7(13)	0.007 7(0)	0.009 4(0)	0.026 4(0)	−0.003 5(0)	−0.005 6(0)	−0.006 3(0)
C(15)	1.341 8(8)	0.483 1(6)	0.797 2(12)	0.009 9(0)	0.006 3(0)	0.023 3(0)	−0.000 6(0)	−0.007 3(0)	−0.008 2(0)
C(16)	1.228 1(7)	0.412 1(6)	0.835 7(10)	0.009 4(0)	0.005 0(0)	0.017 4(0)	0.002 0(0)	−0.007 6(0)	−0.006 6(0)
C(17)	0.143 7(8)	−0.089 3(6)	0.316 4(13)	0.009 3(0)	0.005 3(0)	0.033 0(0)	−0.003 3(0)	−0.005 0(0)	−0.001 4(0)
C(18)	0.731 8(8)	0.582 8(6)	0.681 0(12)	0.009 5(0)	0.005 9(0)	0.023 5(0)	0.006 0(0)	−0.012 2(0)	−0.002 5(0)
H(1)	0.395(9)	0.666(7)	0.237(13)	8.000 0(0)					
H(2)	0.390(11)	0.716(9)	0.061(15)	8.000 0(0)					
H(3)	0.57(8)	0.218(7)	0.083(12)	8.000 0(0)					
H(4)	0.398(6)	0.226(5)	0.657(9)	8.000 0(0)					
H(5)	0.829(7)	−0.169(6)	0.298(10)	8.000 0(0)					
H(6)	0.882(9)	0.037(7)	0.160(12)	8.000 0(0)					
H(7)	0.228(7)	0.123(5)	0.226(10)	8.000 0(0)					
H(8)	0.139(0)	0.832(0)	0.393(0)	8.000 0(0)					
H(9)	1.241(8)	0.331(6)	0.927(11)	8.000 0(0)					
H(10)	1.415(9)	0.649(7)	0.646(13)	8.000 0(0)					
H(11)	0.204(7)	0.711(6)	0.619(10)	8.000 0(0)					
H(12)	0.183(6)	0.588(5)	0.165(9)	8.000 0(0)					
H(13)	0.109(0)	0.971(0)	0.213(0)	8.000 0(0)					
H(14)	0.723(0)	0.168(0)	0.145(0)	8.000 0(0)					
H(15)	0.750(0)	0.668(0)	0.607(0)	8.000 0(0)					
H(16)	0.305(0)	0.471(0)	0.355(0)	8.000 0(0)					
H(17)	1.443(0)	0.471(0)	0.820(0)	8.000 0(0)					
H(18)	0.277(0)	0.832(0)	0.855(0)	8.000 0(0)					
H(19)	0.055(0)	0.193(0)	0.105(0)	8.000 0(0)					
H(20)	0.277(0)	0.389(0)	0.428(0)	8.000 0(0)					

The form of the anisotropic thermal parameter is $\exp\{-[B(1,1)hh + B(2,2)kk + B(3,3)ll + B(1,2)hk + B(1,3)hl + B(2,3)kl]\}$.

Table 4. Important bond lengths (Å) and angles (°)

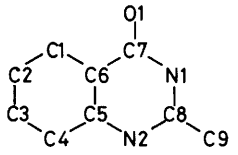

(IV)

Average aromatic C–C 1.388(6) Å
Average aromatic C–C–C angle 120.0(4)°

C(6)–C(7)	1.453	C(7)–N(1)–C(8)	122.7
C(7)–O(1)	1.247	N(1)–C(8)–N(2)	123.2
C(7)–N(1)	1.369	C(8)–N(2)–C(5)	118.0
C(5)–N(2)	1.386	N(2)–C(5)–C(6)	123.0
N(2)–C(8)	1.282	C(5)–C(6)–C(7)	117.4
C(8)–C(9)	1.479	C(6)–C(7)–N(1)	115.7
N(1)–C(8)	1.390	C(6)–C(7)–O(1)	123.9
		N(1)–C(7)–O(1)	120.5
		N(1)–C(8)–N(2)	123.2

E.s.d.s 0.005—0.008 Å, 0.3—0.4°.

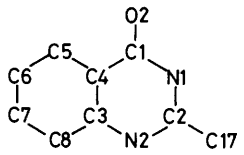

(III)

Molecule A

Average aromatic C–C 1.388(8) Å
Average aromatic C–C–C angle 120.0(5)°

C(4)–C(1)	1.447	C(1)–N(1)–C(2)	123.4
C(1)–O(2)	1.223	N(1)–C(2)–N(2)	124.1
C(1)–N(1)	1.389	C(2)–N(2)–C(3)	116.6
C(3)–N(2)	1.401	N(2)–C(3)–C(4)	123.2
N(2)–C(2)	1.283	C(3)–C(4)–C(1)	118.7
C(2)–C(17)	1.528	C(4)–C(1)–N(1)	114.0
N(1)–C(2)	1.375	C(4)–C(1)–O(2)	126.8
		N(1)–C(1)–O(2)	119.2
		N(1)–C(2)–N(2)	123.8

0.007—0.009 Å, 0.5—0.6°.

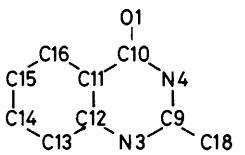

(III)

Molecule B

Average aromatic C–C 1.389(8) Å
Average aromatic C–C–C 120.0(5)°

C(11)–C(10)	1.460	C(10)–N(4)–C(9)	125.4
C(10)–O(1)	1.222	N(4)–C(9)–N(3)	123.2
C(10)–N(4)	1.366	C(9)–N(3)–C(12)	116.7
N(3)–C(12)	1.397	N(3)–C(12)–C(11)	122.8
N(3)–C(9)	1.287	C(12)–C(11)–C(10)	119.2
C(9)–C(18)	1.484	C(11)–C(10)–N(4)	112.7
N(4)–C(9)	1.379	C(11)–C(10)–O(1)	126.6
		N(4)–C(10)–O(1)	120.8
		N(4)–C(9)–N(3)	123.4

0.007—0.009 Å, 0.5—0.6°.

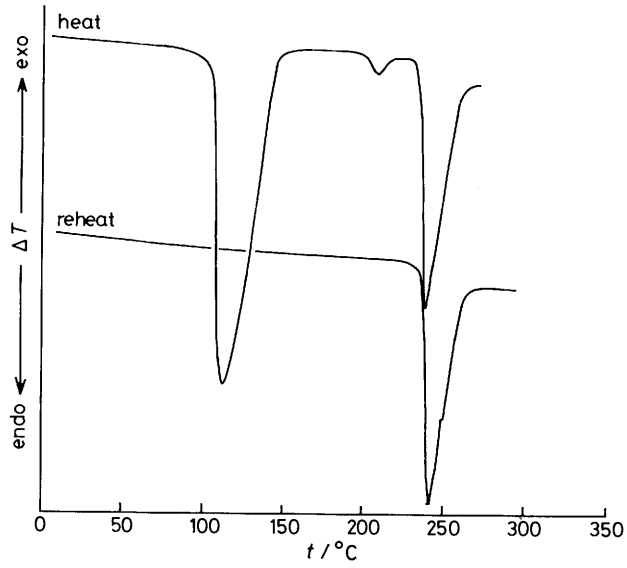

Figure 2. D.t.a. spectrum, run on a Dupont 900 differential thermal analyser at a heating rate of 30 °C min^{-1}, of the quinazolone hydrate (E) showing the endotherm due to loss of water between 100 and 150 °C. The small endotherm at 210 °C is as yet unexplained. After cooling and reheating, the only endotherm which is left is that due to melting of the anhydrous quinazolone (D)

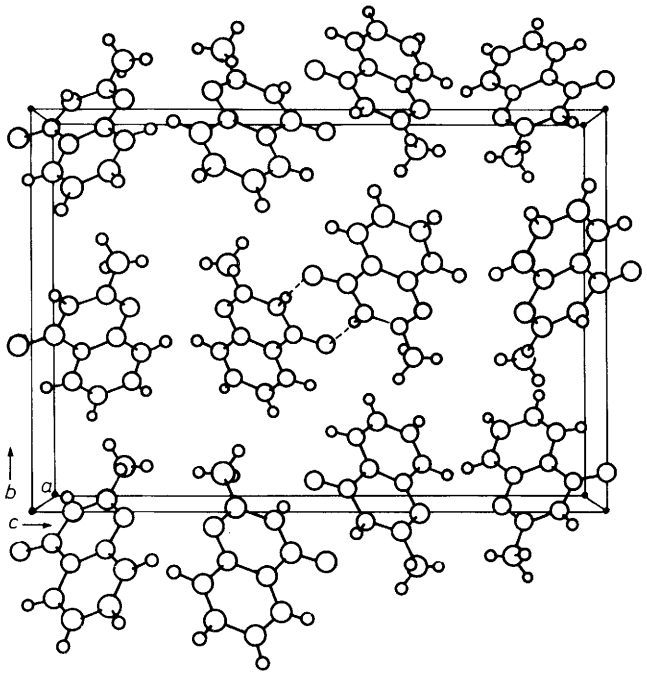

Figure 3. Crystal packing pattern of the anhydrous quinazolone (D) viewed along [100] showing the i-related hydrogen-bonded dimers packing in stacks parallel to the *b*-axis

isolated from this sample are of two types only, one of which matches the patterns of (B) and one of which matches those of (E). I.r. analysis of the bulk sample showed the presence of (B) only. To check the sensitivity of this technique, mixed samples of (B) and (D) were prepared in varying proportions. It was found that qualitatively one could not detect (D) in concentrations <25%. Fourier transform i.r. techniques did show that there are small amounts of (D) (<10%) present in the

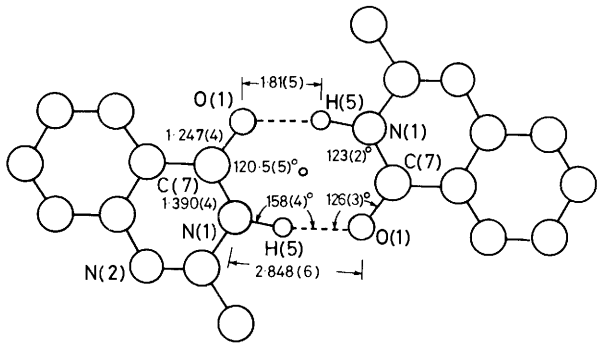

Figure 4. Calculated interat omic distances and angles in the hydrogen-bonded dimers of the anhydrous quinazolone (D)

sample. There was no evidence in the Fourier transform i.r. spectra for bands due to (E). Thus (F) is a solid-state species with a reduced m.p. which contains *ca.* 90% (B) and 10% (D).

Results and Discussion

Crystal Structure Analyses.—The observed bond lengths and angles found for (IV) are consistent with the expected geometry showing a localized N(2)–C(8) double bond and no evidence for tautomeric structures. The packing pattern, shown in Figure 3, consists of inversion related hydrogen-bonded dimers, such as those frequently found for primary amides. Leiserowitz has demonstrated that secondary amides usually exist in a *trans*-conformation in the solid state which gives rise to polymeric hydrogen-bonded chains.[2] In (IV), however, the amide is fixed in a *cis*-conformation which allows dimers to form. The geometry of the dimer is shown in Figure 4. These dimers pack into the orthorhombic cell in stacks such that there are alternating hydrophobic and hydrophilic planes parallel to (001).

Compound (III) packs in an entirely different structure than (IV); nevertheless the intramolecular geometry of both molecules in the asymmetric unit is remarkably similar to that of (IV) (see Table 4). The two independent quinazolone molecules and both water molecules in the asymmetric unit of (III), are involved in a full three-dimensional hydrogen-bonded network, shown in Figure 5. The quinazolone molecules in the asymmetric unit are associated by way of a water molecule which is hydrogen bonded to the amide hydrogen of one molecule and to the imide nitrogen of the other [O(3) · · · HN(4), O(3)H · · · N(2)]. This water molecule also bonds to the carbonyl oxygen of an inversion related molecule [O(3)H · · · O(2)]. The second water molecule is involved in a trigonal hydrogen-bonding scheme, whereby O(4) bonds to the amide N(1)H within the asymmetric unit as well as to O(1) and N(3) in two different inversion related molecules, shown in Figure 6.

Solid-state Reactions.—There are three thermal solid-state reactions (i)—(iii) which have been studied here. The latter two were studied in an effort to identify the chemical nature of (C).

$$(B) \longrightarrow (C) \longrightarrow (D) \quad \text{(i)}$$

$$(E) \longrightarrow (D) \quad \text{(ii)}$$

$$(F) \longrightarrow (D) \quad \text{(iii)}$$

Reaction (i) involves simultaneous intramolecular cycloaddition, molecular dehydration, and solid-state dehydration to give (D) in the form of microcrystallites. The identity of the intermediate (C) is crucial to understanding the solid-state

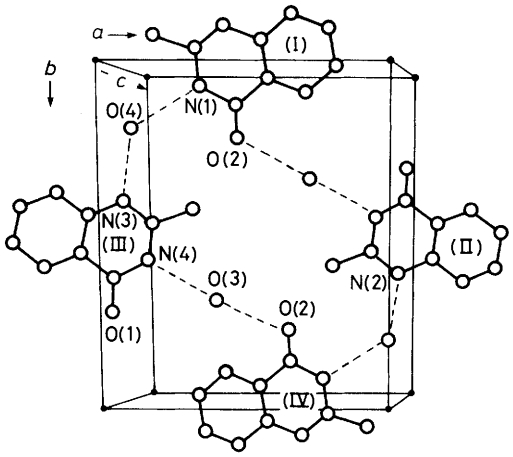

Figure 5. Crystal packing pattern of the quinazolone hydrate (E) viewed along [001], showing the hydrogen-bonding network involving the four molecules of the unit cell [molecules (I) and (II) are the two independent molecules in the asymmetric unit; (III) and (IV) are the inversion related pair at $1 - x$, $1 - y$, $1 - z$]. O(3) and O(4) each have one additional hydrogen bond, shown in Figure 6

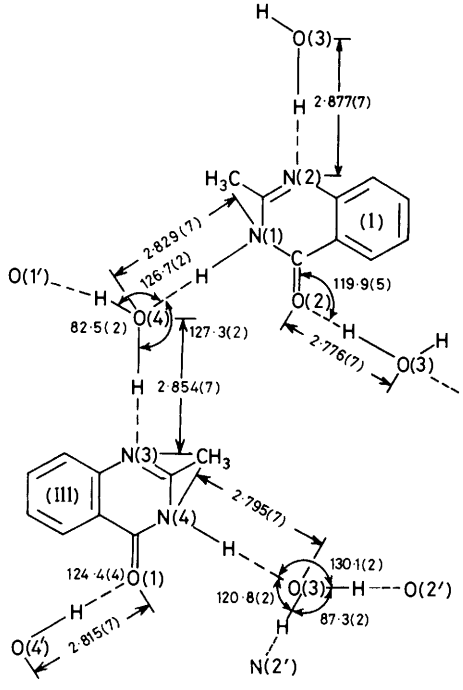

Figure 6. The geometry of the water molecules in the hydrogen-bonded network of the quinazolone hydrate (E). O(1′) is from molecule (II), translated by one unit cell length in the *c* direction. N(2) is from molecule (I) translated by one unit cell length in the *b* direction. O(2′) is from molecule (IV)

processes involved in the conversion (B) ⟶ (D). It was of interest to determine whether (C) corresponded to (III), or its crystal form (E). We found no evidence for the presence of either, although undoubtedly (III) has formed as a transient species. Likewise, we could find no evidence for significant quantities of an alcohol (II).

The first clue to the identity of (C) came from the observation that on occasion a solid (F) with unusual solid-state

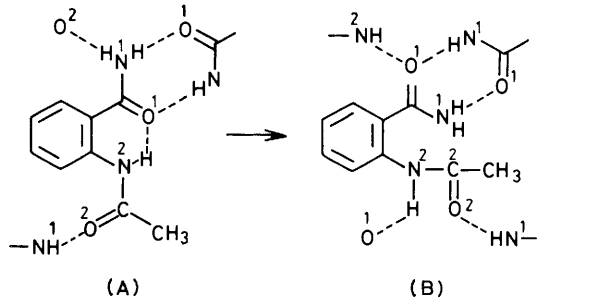

properties could be obtained from recrystallization of (I) in basic solution. The composition of (F) was elusive, but its thermal properties were reproducible and were remarkably similar to those of (C). It was found that (a) the i.r. spectrum of (F) showed the sample to be mainly (I), containing 10% or less of (IV), (b) (F) has a reduced m.p. compared with (B) and (D), and (c) several crystals of (F) gave *X*-ray patterns matching those of (B). In conjunction with the knowledge that a eutectic compound composed of (I) and (IV) had been isolated from solution and characterized by Errede,[4] the solid-state properties of (F) strongly suggest that it may be a mixture of the eutectic form and either (B) or a solid solution of (B) and (D) with a crystal packing pattern similar to that of (B). What is unusual here is that the composition of (F) is changing during melting. As the concentration of (IV) builds up, re-solidification of the melt takes place, followed by remelting at the m.p. of D. This process is shown in Scheme 2.

$$\text{F} \xrightarrow[160\ ^\circ\text{C}]{-H_2O} \text{melt} \xrightarrow[170\ ^\circ\text{C}]{} \text{solid} \xrightarrow[240\ ^\circ\text{C}]{} \text{melt}$$

$$[(I)] \gg [(IV)] \qquad [(I)] > [(IV)] \qquad [(I)] < [(IV)] \qquad (IV)$$

Scheme 2

A similar process is proposed for reaction (i) in which (C) is dehydrated to give (D). In that case, (C), formed as an intermediate during the solid-state cyclodehydration of (I), most likely contains the reaction product (IV) trapped in the lattice of (B). Further heating of the solid leads to complete conversion into (IV), and dehydration of the solid to give (D).

Role of the Hydrogen-bonding Network.—Errede has suggested that hydrogen-bonding patterns in the local environment of a reacting centre can influence the rates and even the product distribution of ammonolysis and hydrolysis reactions in solution.[5] His work shows that local ordering of water molecules may be responsible for the curious fact that (I) readily cyclodehydrates to give (IV) in water solution, contrary to the law of mass action. The course of the solid-state dehydration (I) ⟶ (IV) also depends on the hydrogen-bonding patterns in the reaction matrix. In this reaction sequence there are three distinct steps: the polymorphic transformation (A) ⟶ (B), formation of an intermediate solid phase as (B) begins to react and form (C), and finally phase separation of anhydrous product (D) (Scheme 1).

For (A) ⟶ (B), the only hydrogen bond which needs to change is an intramolecular N(2)H · · · O(1) bond which breaks and reforms as an intermolecular N(2)H · · · O(1) bond between the same atoms but on neighbouring molecules.[3] Compound (B) is in a conformation in which the reacting centres N(1) and C(2) are aligned in a geometry which would favour reaction (even though they are not within reacting distance before heating).

Species (B) has three intermolecular bonds, N(1)H · · · O(1), N(1)H · · · O(2), and N(2)H · · · O(1). As cyclodehydration takes place N(1)H · · · O(2) and N(2)H · · · O(1) must break

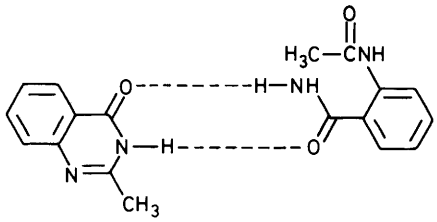

(V)

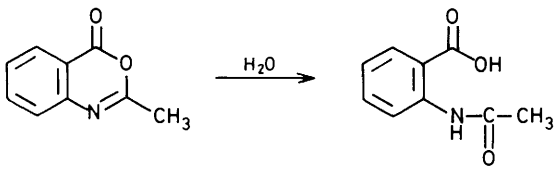

(VI)(G) (VII)

since those two protons and O(2) are lost as water is formed. The only hydrogen bond which would be left in (B) as it reacts is the cyclic amide dimer bond formed between N(1)H and O(1) on inversion related molecules. The product (D) also has this dimer pair as its only hydrogen-bonding interaction. In fact, the dimer interaction occurs in the entire sequence from (A) to (D) and may be critical for the formation of (C) as an intermediate. During the early stages of the cyclodehydration reaction, (IV) could be trapped in the lattice of (B) in an unsymmetrical dimer arrangement (V), like that found for the complex of 2-pyridone and 6-chloro-2-hydroxypyridine.[6] Further evidence that the dimer interaction may be preserved during the entire reaction sequence is the fact that (E) is *not* found as an intermediate. Species (E) has no cyclic dimer interaction in its structure; all its available hydrogen donor and acceptor sites are hydrogen bonded to water molecules. Thus, in this reaction sequence polymorphic transformations and chemical reactions appear to occur along pathways which preserve the integrity of the cyclic dimer pattern.

In the independent reaction (E) ⟶ (D), cyclic dimers form between quinazolone molecules as water leaves the lattice. Once (D) has formed, the hydrate (E) cannot be reformed in the solid state even under forcing conditions (soaking the product crystals in water solution overnight). Just as when (D) is formed by cyclodehydration of (B), the water molecules do not substitute into the hydrogen-bonding pattern of the cyclic dimers. On the other hand, crystals of the oxygen analogue of (I), (VI) in structure (G), containing no hydrogen bonds at all, are readily attacked by water to give acetylanthranilic acid (VII).[7]

These studies suggest that one may be able to rank relative solid-state ' reactivities ' of different hydrogen-bonding modes, in much the same way that one can predict the solution reactivity of many kinds of molecules by examining the nature of their functional groups. In this context, the solid-state reactions of hydrogen bonds include any process which causes a hydrogen bond to break, *e.g.* polymorphic transformations, chemical reactions, hydrolyses, *etc.* In the series of reactions studied here the relative reactivities of hydrogen bonds (in ascending order of reactivity) would be cyclic hydrogen-bonded dimers > other intermolecular NH · · · O bonds > intramolecular hydrogen bonds > hydrogen bonds involving

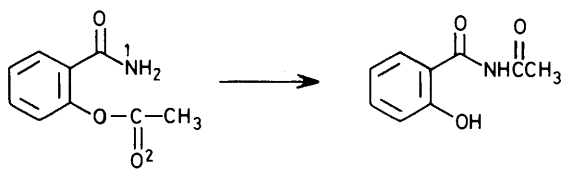

(VIII)(H) (IX)(J)

water. This ranking does not necessarily correlate with individual hydrogen bond strengths, but rather reflects the relative solid-state stabilities of patterns of extended sequences of hydrogen-bonded molecules.

This ranking criterion can be applied to other reactions, for example, *O*-acetylsalicylamide (VIII) isomerizes to *N*-acetylsalicylamide (IX) in a thermal solid-state transformation (H) ⟶ (J).[8] Manohar has recently reported preliminary studies on the mechanism of this reaction and the crystal structures of (VIII) and (IX).[9] The structure of (VIII) in (H) is very similar to that of (Iβ) in (B), having two of the same hydrogen-bonding patterns present in (B). The ranking given above suggests that during the thermal rearrangement of (H) the N(1)H · · · O(2) bond would break first and the dimer bonds would break last.

In the hydrogen-bonded systems studied here, product molecules form in such a way that a hydrogen-bonding network can be maintained as the different reaction stages take place, even though the hydrogen-bonding patterns are changing. The nature of the hydrogen-bonding network in the reagent may dictate not only what chemical intermediates will form, but also which polymorph of the product will be nucleated. Our current efforts are directed at testing these possibilities on related reactions in hydrogen-bonded solids.

Acknowledgements

Helpful discussions and critical input provided by Professors G. Christoph, Ohio State University, and D. Y. Curtin, University of Illinois, and the laboratory assistance of D. Bradley, Saint Paul Academy High School, are gratefully acknowledged. The assistance of 3M analytical personnel is also appreciated.

References

1 Part 1, L. A. Errede, M. C. Etter, R. C. Williams, and S. M. Darnauer, *J. Chem. Soc., Perkin Trans. 2*, 1981, 233.
2 L. Leiserowitz and M. Tuval, *Acta Crystallogr.*, 1978, **B34**, 1230.
3 L. Leiserowitz and G. M. J. Schmidt, *J. Chem. Soc. A*, 1968, 2372.
4 L. A. Errede, P. D. Martinucci, and J. J. McBrady, *J. Org. Chem.*, 1980, **45**, 3009.
5 B. A. Frenz, ' Enraf-Nonius Structure Determination Package,' Molecular Structure Corporation, College Station, 1978, 3rd edn.
6 J. Almlof, A. Kvick, and I. Olovsson, *Acta Crystallogr.*, 1971, **B27**, 1201.
7 M. C. Etter and J. Vicens, *Cryst. Struct. Commun.*, in the press.
8 A. J. Gordon, *Tetrahedron*, 1967, **23**, 863.
9 V. Mohan Rao and H. Manohar, Abstr. 04.4-06, 12th IUCr Meeting, Ottawa, 1981.

Received 23*rd March* 1982; *Paper* 2/503